J. Geophys. 45, 281–298, 1979

Journal of Geophysics

Analysis of an Eastward Electrojet by Means of Upward Continuation of Ground-Based Magnetometer Data

U. Mersmann, W. Baumjohann, F. Küppers, and K. Lange

Institut für Geophysik der Universität Münster,
Gievenbecker Weg 61, D-4400 Münster, Federal Republic of Germany

Abstract. On October 26, 1975, data from two parallel meridian chains of densely spaced magnetometers in Northern Scandinavia indicated the presence of an evening sector eastward electrojet which between 1606 and 1710 UT was two-dimensional. By separating the relevant components of the magnetic disturbance fields into internal and external parts, and by subsequent upward continuation (towards the source) of the external horizontal component, equivalent height-integrated ionospheric current densities were derived as a function of latitude and time. Whereas the demarcation line between the eastward and westward ionospheric electrojet currents remained stationary, the sharp southern border of the eastward electrojet moved towards the south with a speed of about 50 ms^{-1}, possibly indicating an earthward movement of the inner edge of the magnetospheric plasma sheet. The maximum eastward height-integrated current density was of the order of 0.5 Am^{-1}, the corresponding large-scale field-aligned current density has been estimated to have been of the order of 1.0 μAm^{-2}. After 1630 UT there was evidence for a superposed stationary small-scale structure (wavelength of the order of 250 km) in the eastward flow, which would imply a pair of local field-aligned current sheets possibly related to an auroral arc.

Key words: Magnetic variations – Scandinavian magnetometer array – Field separation – Upward continuation of external fields – Eastward auroral electrojet – Field-aligned currents.

Introduction

It is well known that during periods of enhanced magnetospheric activity an eastward electrojet flows in the dark postnoon and evening sector along the southern part of the auroral oval (Kamide and Fukushima, 1972; Rostoker, 1972) simultaneously with a more poleward situated westward electrojet, which

0340-062X/79/0045/0281/$03.60

penetrates from the midnight into the evening sector during periods of substorm activity (Rostoker and Kisabeth, 1973; Rostoker et al., 1975). The eastward electrojet flows in a conductivity channel generated mainly by diffuse and relatively uniform precipitation (Wallis et al., 1976) of inner plasmasheet particles (Lui et al., 1977). It is driven by a northward electric field, which has been observed by means of satellites (e.g. Maynard, 1974), rockets (e.g., Evans et al., 1977) and the Chatanika-radar (e.g., Banks et al., 1973). Field-aligned currents appear to flow upward in the poleward and downward in the equatorward half of the eastward electrojet region (Rostoker et al., 1975). Therefore it may be assumed that the eastward electrojet mainly consists of a relatively uniform – if compared with the substorm westward electrojet – Hall current (Wescott et al., 1969; Brekke et al., 1974; Baumjohann et al., 1978).

Besides these large-scale features, small-scale phenomena have also been observed in the eastward electrojet region most of which are related to auroral arcs. Wallis et al. (1976) and Wallis (1976) observed auroral arcs embedded in the region of diffuse aurora. Lui et al. (1977) reported highly structured and intense electron precipitation causing discrete auroras sometimes embedded in the diffuse precipitation aurora region and Mende and Eather (1976) found dynamic structures in the soft and mainly diffuse electron precipitation. Iijima and Potemra (1978) observed fine scale structures in the evening sector field-aligned currents during active periods when the westward electrojet had intruded into the evening sector. Armstrong et al. (1975) and Kamide and Rostoker (1977) pointed out that small-scale structures in the field-aligned current flow observed by the TRIAD satellite were related to discrete arcs in the poleward half of the eastward electrojet region. Casserly and Cloutier (1975) found a small-scale field-aligned current sheet pair near an auroral arc in the positive bay region. Maynard et al. (1977) and Evans et al. (1977) reported a decrease of the northward electric field in the eastward electrojet region when their rocket flew over an auroral arc. Beaujardiere et al. (1977) observed southward electric fields in evening arcs, which were embedded in an ambient northward electric field, using data from the incoherent scatter radar at Chatanika.

At the present we have tried to apply the method of field continuation towards the source to ground-based magnetic observations of an eastward electrojet. This method is well-known in applied geophysics (see e.g., Grant and West, 1965) and has been already used by McNish (1938) in order to estimate possible heights of auroral zone ionospheric currents. These results were much limited by the large mutual distances and the irregular distribution of magnetic observation stations. Against this we were able to base our investigation on two parallel, closely neighbouring profiles which were rather evenly and densely occupied by magnetometers.

As compared to methods where, in the course of interpolation, model ionospheric or magnetospheric current systems are adjusted to ground-based magnetic observations by trial and error or some inversion techniques, the method of upward continuation presents a rather direct way by which at least equivalent height-integrated ionospheric current densities can be derived. It was the main purpose of the present study to examine this method in practice for a two-dimensional case in which variability transverse to the profiles of observations

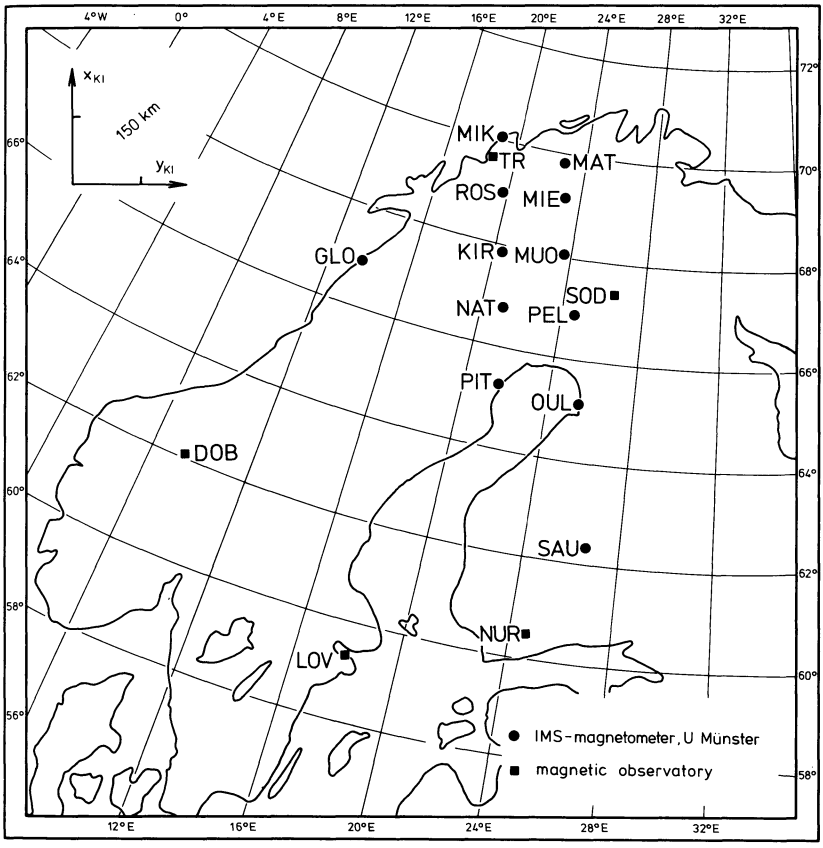

Fig. 1. Locations of magnetic stations used in this study. Within the *upper left corner* the Kiruna system (see text) is indicated, besides its origin which is at Kiruna (*KIR*)

might be neglected, and accordingly a two-dimensional algorithm could be applied.

Instrumentation

During the International Magnetospheric Study (IMS) the University of Münster is operating an array of magnetometers of an improved Gough-Reitzel type (Gough and Reitzel, 1967; Küppers and Post, 1979) in Scandinavia (Küppers et al., 1979). In 1975 13 of these magnetometers, on two nearly parallel profiles aligned along geomagnetic meridians with a spacing of 100–150 km in northern Scandinavia, were already recording. Also an additional one was operating at the western coast of northern Norway. Data from 12 of these stations, as shown in Fig. 1, were available for October 1975 and have been used together with data from the magnetic observatories shown in the figure and from the two observatories Bear Island (BJO, 74.5°N, 19.0°E) and Ny Alesund (NAL, 78.9°N, 11.9°E), which are located further to the north.

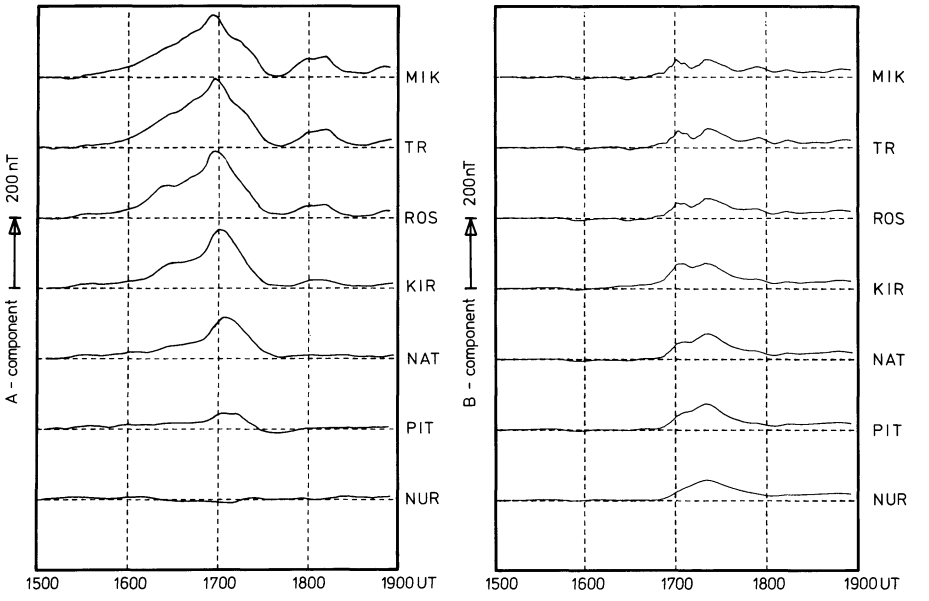

Fig. 2. Magnetograms of lowpass-filtered *A*- and *B*-components for the western profile of magnetometers (see Fig. 1), on October 26, 1975. The *A*- and *B*-components are defined parallel to the x_{KI}- and y_{KI}-axis, respectively (cf. Fig. 1)

The coordinate system indicated in the upper left corner of Fig. 1 has been introduced by Küppers et al. (1979) and named the Kiruna system. It is a Cartesian system obtained by a stereographic projection of the globe onto a tangential plane centered at Kiruna, Sweden (67.8° N, 20.4° E). Cartesian coordinates are very suitable for analysing magnetic field data by means of potential theory methods as applied in this paper. The y_{KI}-axis of the system has been chosen as the tangent to the projection of the ϕ_c (KIR) = 64.8° line with ϕ_c being the revised corrected geomagnetic latitude as given by Gustafsson (1970). The x_{KI}-axis is perpendicular to the y_{KI}-axis and is directed approximately 12° west of geographic north at Kiruna, where the system has its origin ($x_{KI} = y_{KI} = 0$).

General Character of the Magnetic Variations Observed

On October 26, 1975, a positive bay of about 200 *nT* was observed between 1500 and 1800 UT (1730–2130 MLT) in the Scandinavian sector at a time of weak magnetospheric activity ($Kp = 3$). Variations of the magnetic components *H*, *D*, and *Z* relative to the quiet day level were lowpass-filtered with a simple moving average filter to remove small-scale magnetic variations with periods less than 5 min, which were superimposed on the positive bay signature. The filtered variations were then mapped into the Cartesian Kiruna system.

In Fig. 2 the magnetograms for the lowpass-filtered *A*-components (magnetic deflection parallel to the x_{KI}-axis) and *B*-components (magnetic deflection paral-

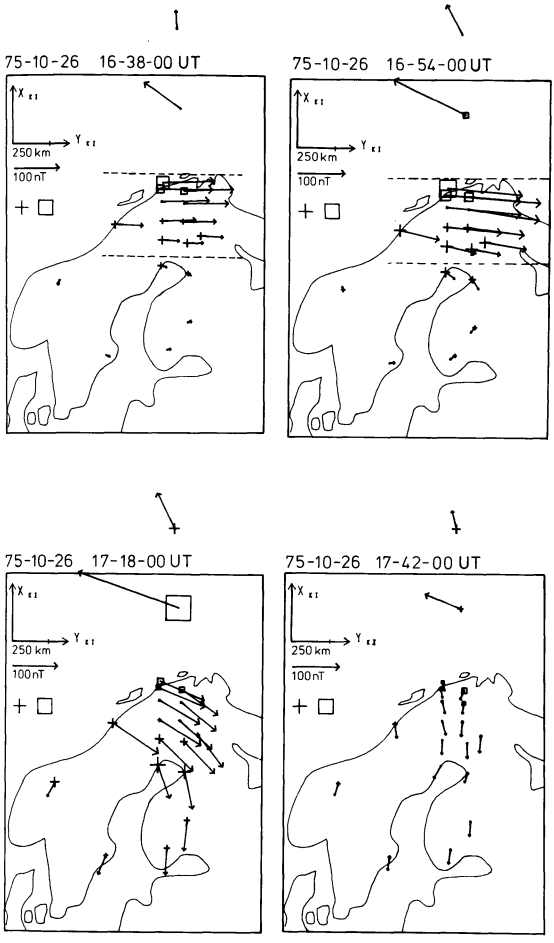

Fig. 3. Equivalent current arrows (in *nT*) on the earth's surface for 4 instances of time. The current arrows have their origin at the station, where the corresponding magnetic disturbances have been recorded. Squares and crosses denote negative and positive *Z*-components, respectively. The *dashed lines in the upper two panels* give the borders of the main two-dimensional equivalent eastward flow

lel γ_{KI}) observed on the western profile of stations are illustrated. Figure 3 shows the equivalent current vectors on the earth's surface at four different times. The equivalent current vector is obtained from the measured horizontal magnetic disturbance vector by rotating the latter vector 90° clockwise, as viewed from above.

Apparently the positive A-perturbation (indicating an eastward electrojet) commences for all stations in northern Scandinavia around 1520 UT. The magnitude increases slowly until 1700 UT, when it reaches its peak value with the largest *A*-values about 100 km south of the northern coast of Norway (stations ROS and MIE). Note that this maximum occurs later at the more southern

and also (not shown in Fig. 2) at the more western stations. This southwestern expansion of the eastward electrojet has also been observed by Kamide and Fukushima (1972). At about 1650 UT the B-perturbation changes from zero to positive, indicating a southward component of the equivalent current flow. From 1650 UT onwards the B-components increase, with their maximum occurring at about 1720 UT while the A-components slowly decrease. This gives rise to a southward turning of the equivalent current flow as seen in the lower two diagrams of Fig. 3.

The small values of B, and the similarity in the A-variations observed at equivalent stations of both profiles, infer that the main part of the current system is rather two-dimensional until 1710 UT. This is supported by the equivalent current vectors plotted in the upper two diagrams of Fig. 3.

Finally it should be noted that the magnetic signatures seen more to the north at BJO show a westward electrojet during the whole interval. This jet penetrated into the evening sector due to substorm activity around midnight (Rostoker and Kisabeth, 1973; Rostoker et al., 1975; Iijima and Potemra, 1978). Magnetograms of Siberian observatories give clear indications of an increase in westward electrojet activity during the interval studied. Especially Cape Chelyuskin showed clear signatures of a substorm onset (cf. Untiedt et al., 1978) by a strong and abrupt decrease in H together with a sudden increase in D when it was located just around magnetic midnight (at about 1645 UT). The northernmost station NAL showed rather northward directed equivalent currents during the whole interval, which seem to be related to polar cap effects (Wallis et al., 1976). Current directions at both stations (BJO and NAL) are not exactly antiparallel to the eastward electrojet flow. This fact together with the rather large spacing made a quantitative analysis of the northern part of the current system impossible. Accordingly, all results for the westward electrojet shown in the next sections should be taken more qualitatively than quantitatively.

Equivalent Height Integrated Ionospheric Current Density Profiles Calculated Via Field Separation and Upward Continuation

For a two-dimensional analysis of the equivalent current system between 1606 and 1710 UT it was necessary to construct latitude profiles of the horizontal and vertical magnetic components perpendicular to the main current direction. Therefore, separately for each instance of time, both spatial (x_{KI}, y_{KI}) and magnetic horizontal (A, B) coordinate axes of the Kiruna system have been rotated by the average of the local angles $\alpha_i(t) = \tan^{-1}[B_i(t)/A_i(t)]$ given by stations under the main current flow (e.g., stations between the two dashed lines in the upper two diagrams of Fig. 3). This minimized the variations in the horizontal component parallel to the jet and yielded the new horizontal magnetic component V, along the new u_{KI}-axis, perpendicular to the eastward electrojet. In the upper part of Fig. 4, latitude profiles constructed by cubic spline interpolation of the V- and Z-components along the u_{KI}-axis for the magnetic field observed on the western profile at 1638 UT are illustrated. Also shown is the magnetic component parallel to the main current direction (W, dotted line

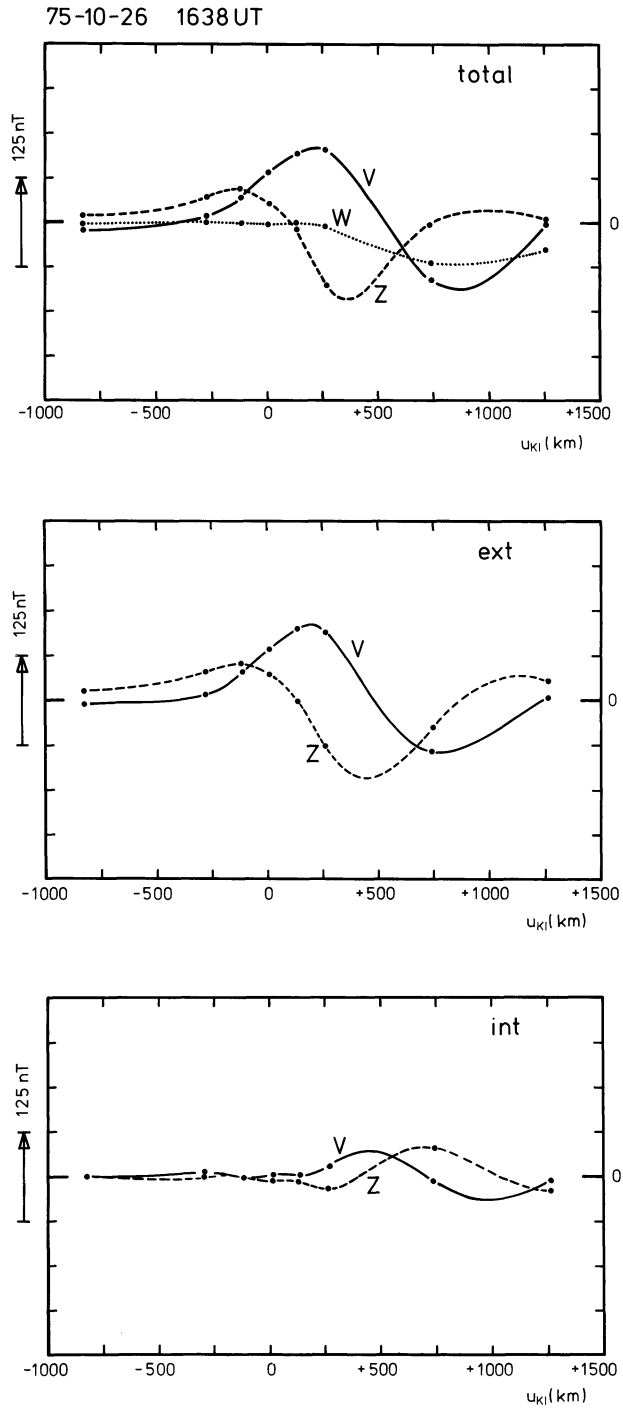

Fig. 4. Latitude profiles of observed (*upper diagram*), external (*middle diagram*) and internal (*lower diagram*) magnetic field components for the western chain at 1638 UT. The solid line gives the horizontal *V*-component (perpendicular to the main current flow), the *dashed line* represents the vertical *Z*-component and the *dotted line* in the upper diagram shows the horizontal magnetic component perpendicular to *V* and parallel to the main current flow (*W*). The big dots denote the position of the stations

in the upper diagram). It can be seen that the variations of this component are essentially zero over the Scandinavian mainland. The latitude profiles constructed with stations on the eastern chain are in excellent agreement and support very strongly the idea that a two-dimensional analysis is possible for this time interval, if one keeps in mind that any results for the westward electrojet indicated by the two northern stations are quite ambiguous because of the deviating current direction and the great spacing between these stations.

Since the magnetic field observed on the ground is a superposition of the ionospheric-magnetospheric source field and the field of the currents induced in the ground, it appeared to be necessary to separate the magnetic horizontal component V and the vertical component Z into inner and outer parts. For a two-dimensional case in a Cartesian coordinate system this can be achieved by means of the Hilbert transform (Kertz, 1954; Siebert and Kertz, 1957; Weaver, 1964). With the Kertz operator K defined by:

$$KF(u_{\mathrm{KI}}) = \frac{1}{\pi} \int_{-\infty}^{+\infty} \frac{F(\hat{u}_{\mathrm{KI}})}{u_{\mathrm{KI}} - \hat{u}_{\mathrm{KI}}} d\hat{u}_{\mathrm{KI}}$$

one gets the following relations for the internal and external parts of the magnetic field on the earth's surface:

$$\begin{aligned}
V_e(u_{\mathrm{KI}}) &= \tfrac{1}{2}[V(u_{\mathrm{KI}}) + KZ(u_{\mathrm{KI}})] \\
V_i(u_{\mathrm{KI}}) &= \tfrac{1}{2}[V(u_{\mathrm{KI}}) - KZ(u_{\mathrm{KI}})] \\
Z_e(u_{\mathrm{KI}}) &= \tfrac{1}{2}[Z(u_{\mathrm{KI}}) - KV(u_{\mathrm{KI}})] \\
Z_i(u_{\mathrm{KI}}) &= \tfrac{1}{2}[Z(u_{\mathrm{KI}}) + KV(u_{\mathrm{KI}})].
\end{aligned}$$

Since the integral has to be calculated from $-\infty$ to $+\infty$ one has to assume extrapolating functions for the V and Z latitude profiles outside the data interval. In the present analysis an exponential trend was matched at the data of the northern and southern limits of the profiles. This trend function slowly decreased to zero with increasing distance from the limits.

The separated fields for 1638 UT are illustrated in Fig. 4, where the middle panel shows the external parts of the magnetic components given in the upper part and the lower diagram gives the internal parts. It is seen quite clearly that the field due to induced currents seems to be rather weak over the Scandinavian mainland ($u_{\mathrm{KI}} < +200$ km) while it appears to increase over the sea. Either the poor two-dimensionality of the westward jet or the good conducting seawater could possibly be responsible for the different positions of extrema respectively zero-crossovers of external and internal parts. For a more detailed discussion of this topic see Küppers et al. (1979).

If the external magnetic horizontal component V_e is assumed to be periodic along the u_{KI}-axis, with $2\pi k_0^{-1}$ defining the basic wavelength (large as compared to the length of our profiles) it may be expanded below the ionosphere according to potential theory into the series:

$$V_e(u_{\mathrm{KI}}, z) = \sum_{n=0}^{\infty} (a_k \cos(k u_{\mathrm{KI}}) + b_k \sin(k u_{\mathrm{KI}})) e^{kz}$$

where $k = nk_0$ denotes the wavenumber and z denotes the height.

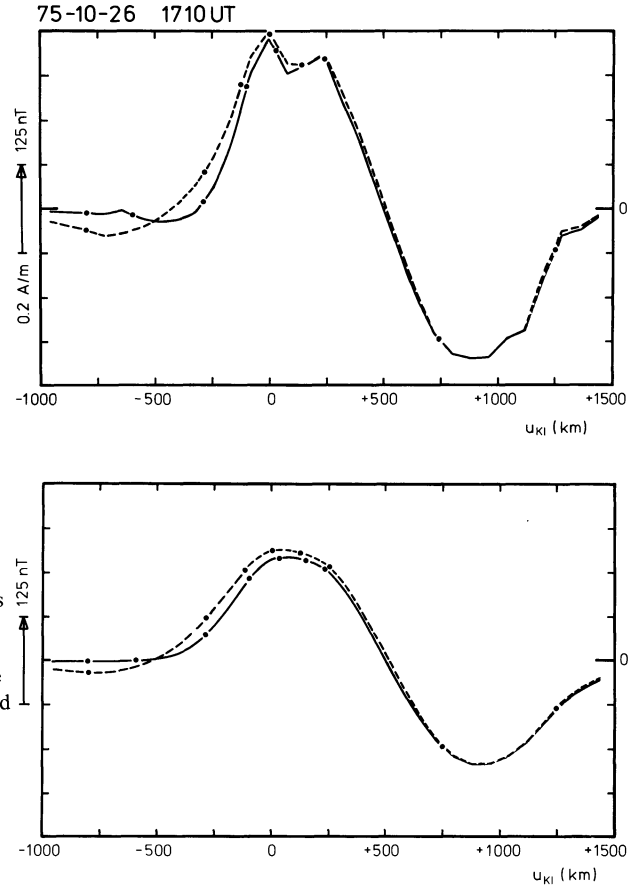

Fig. 5. Latitude profiles of the external horizontal magnetic V component (cf. Fig. 4) for both chains of stations at 1710 UT. The lower diagram gives the components at the earth's surface while the *upper panel* shows the derived V components at 110 km height or the equivalent height-integrated eastward ionospheric current density. The *solid line* is representative for the eastern, the *dashed line* for the western chain of stations and the *dots* denote positions of the stations

Therefore Fourier analysis of the V_e latitude profile on the ground, multiplication of the Fourier coefficients with e^{kh} (h assumed height of ionospheric current layer) and subsequent Fourier synthesis yields the magnetic field just below the ionospheric current layer. We have chosen $h=110$ km according to the observed average height of eastward and westward electrojets (Kamide and Brekke, 1977).

During upward continuation, larger wave-numbers, i.e., very large factors e^{kh} lead to the well-known problem of instability of the method (large short-wavelength oscillations of the continued field). The problem may be solved either by cutting the Fourier spectrum above a certain k-value, or by performing a harmonic analysis and synthesis with sufficiently large spacing Δu_{KI} between neighboured field values instead of the above described Fourier analysis of a continuous function. In our case we proceeded along the second line. We found that with $\Delta u_{KI}=80$ km oscillations of the continued field could be avoided, while the spatial resolution was still sufficient and corresponded to a minimum wavelength of 160 km. As an example of the results, the height-continued V_e-component along both magnetometer profiles at 1710 UT is shown in Fig. 5, together with the V_e (u_{KI}) curves on the ground.

From Biot-Savart's law the following relation can be derived for the current density J_{eq} (in Am^{-1} positive eastwards) of the equivalent height-integrated ionospheric current perpendicular to the u_{KI}-axis generating the magnetic component V_e:

$$J_{eq}(u_{KI}) = \frac{2}{\mu_0} V_e(u_{KI}, h)$$

where it is assumed that V_e is given in T. Accordingly, in Fig. 5 (upper part) the height-continued V_e-component may be considered as a height-integrated current density (c.f., corresponding scale to the left).

As compared to the curves given at ground (lower part of Fig. 5), $V_e(u_{KI})$ at 110 km height (upper part of Fig. 5) is more concentrated and shows larger extremum values, as is to be expected after continuation towards the source. Note, however, that the results for $u_{KI} \geqq +300$ km (i.e., especially for the regime of the westward electrojet) are rather ambiguous, because of the reasons mentioned above. Besides an interesting steepening of the southward flank of the eastward electrojet part of the curves during upward continuation, the appearance of a small scale structure near the V_e maximum is quite conspicuous. It corresponds mainly to a wavelength of nearly 250 km, with the above mentioned factor e^{kh} amounting to about 20. Accordingly, this local structure does not appear as an indentation at ground but only as a slight asymmetry within the curve near its maximum.

Of course, it has to be examined if this small-scale structure is real or if it has been introduced artificially in the course of the different mathematical procedures which have been applied. We exclude the possibility that the structure is due to the above mentioned instability of the continuation method, because the corresponding short-wavelength oscillations disappeared rather uniformly along the whole profile when we enlarged the spacing Δu_{KI} stepwise from 20 to 80 km. Also the special interpolation which has been used seems not to be of importance because we got nearly the same indentation for both our profiles though the distribution of stations is clearly different for them. Furthermore, from our experience in a few other similar cases (as communicated privately to us by König and Sulzbacher) the interesting small scale structures do not always appear. This also seems to exclude the possibility that this irregularity is generated from a conductivity anomaly (coast effect, for example) via a not complete separation of internal and external parts. We therefore conclude that it is justified to assume the physical reality of the discussed small-scale structure.

In order to illustrate the temporal behaviour in Fig. 6, the derived equivalent height-integrated eastward current densities are given for 9 instances of time in the 1606 to 1710 UT interval, for which a two-dimensional analysis is considered valid. Apparently, both eastward and westward flowing currents grow steadily until 1702 UT. The maximum equivalent current densities of the eastward electrojet increase from 0.1 Am^{-1} at 1606 UT up to 0.5 Am^{-1} at 1702 UT and the total equivalent eastward current is also enhanced by a factor of 5 from $4 \cdot 10^4$ A to $2 \cdot 10^5$ A during the same interval. Simultaneously with the

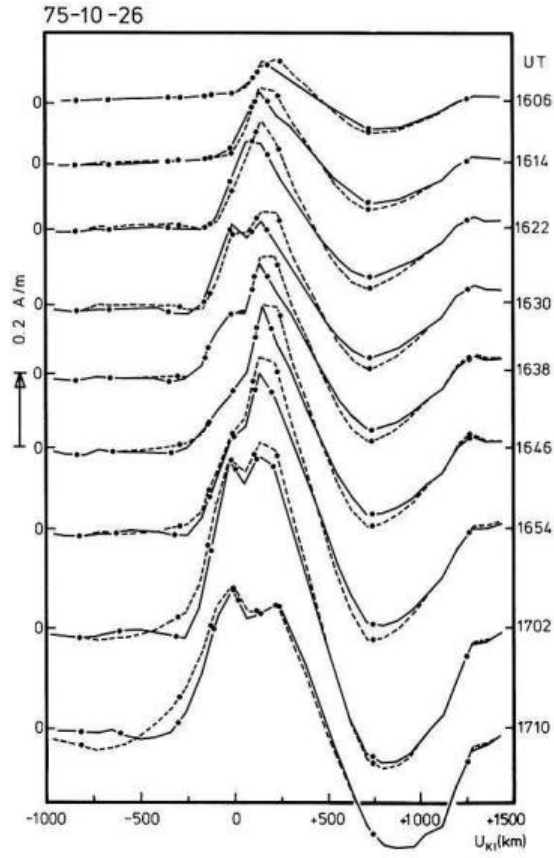

Fig. 6. Latitude profiles of the equivalent height-integrated ionospheric current density for every eighth minute between 1606 and 1710 UT. Otherwise as Fig. 5

growing current amplitude the whole current system broadens. The width of the eastward current system is increased from 500 to 800 km by an equatorward shift of its well-defined southern edge linearly with time (about 50 ms^{-1}), while the demarcation line to the westward flowing current remains stationary at $u_{KI}=500$ km (approximately 69° revised corrected geomagnetic latitude).

Additional to these large-scale features, the above discussed interesting small-scale structure can be seen all the time between 1630 and 1710 UT at a fixed position. It occurs as a local decrease of about 0.1 Am^{-1} near the large-scale current density maximum between $u_{KI}=0$ and 200 km.

Field-Aligned Current Density Profiles

We have also tried to calculate the distribution of field-aligned currents by a method similar to the one used, e.g., by Kamide and Horwitz (1978). The method is based on current continuity:

$$\mathbf{div} \cdot \mathbf{J} = j_{\parallel}$$

and Ohm's law for the ionosphere:

$$\mathbf{J} = \begin{pmatrix} +\Sigma_P & +\Sigma_H \\ -\Sigma_H & +\Sigma_P \end{pmatrix} \cdot \mathbf{E}$$

with $\mathbf{J}$ denoting the horizontal vector of height-integrated ionospheric current density, $j_{\parallel}$ the downward field-aligned current density, Σ_H and Σ_P the height-integrated ionospheric Pedersen- and Hall-conductivity, and $\mathbf{E}$ the horizontal ionospheric electric field (assuming the magnetic field directed vertically downward for high latitudes). If we interpret our equivalent height-integrated ionospheric current density J_{eq} as a Hall-current caused by a pure north-south electric field (e.g., Wescott et al., 1969; Brekke et al., 1974; Zmuda and Armstrong, 1974) we may estimate the downward field-aligned current density by:

$$j_{\parallel}(u_{KI}) = \frac{\partial}{\partial u_{KI}} \left[\frac{\Sigma_P}{\Sigma_H}(u_{KI}) J_{eq}(u_{KI}) \right].$$

The variability of the ratio Σ_H/Σ_P along our profiles and with time is not known. Though results from the Chatanika-radar (see, e.g., Brekke et al., 1974; Horwitz et al., 1978) show that this ratio may vary appreciably with time especially within the regime of the westward electrojet, where it may be as large as 4, a constant value of 2 may be a not too unrealistic estimate for our case of an eastward electrojet (see Brekke et al., 1974; Wedde et al., 1977). With this assumption we get:

$$j_{\parallel}(u_{KI}) = \frac{1}{2} \frac{\partial}{\partial u_{KI}} J_{eq}(u_{KI}).$$

The results of the corresponding calculations are shown in Fig. 7. It shows that the large-scale field-aligned current distribution exhibits downward current flow over a width of 250–500 km in the equatorward half of the eastward electrojet region with current density maxima ranging from $0.4 \cdot 10^{-6}$ to $1.2 \cdot 10^{-6}$ Am^{-2} between 1606 and 1710 UT. The region of field-aligned current flow out of the ionosphere stretches from the poleward half of the eastward electrojet region into the region of the westward electrojet and broadens from 500 to 650 km during the interval studied while the current density maxima increase from 0.3 to $1.0 \cdot 10^{-6}$ Am^{-2}. There is also a poleward region of inflowing field-aligned currents.

The local decrease near the maximum of J_{eq} (cf. Fig. 6) gives rise to a local pair of field-aligned currents of less than 100 km width each (corresponding to the maximum spatial resolution of our analysis). These sheets have maximum current densities of $0.8 \cdot 10^{-6}$ Am^{-2} and $4 \cdot 10^{-2}$ Am^{-1}, respectively, at 1702 UT.

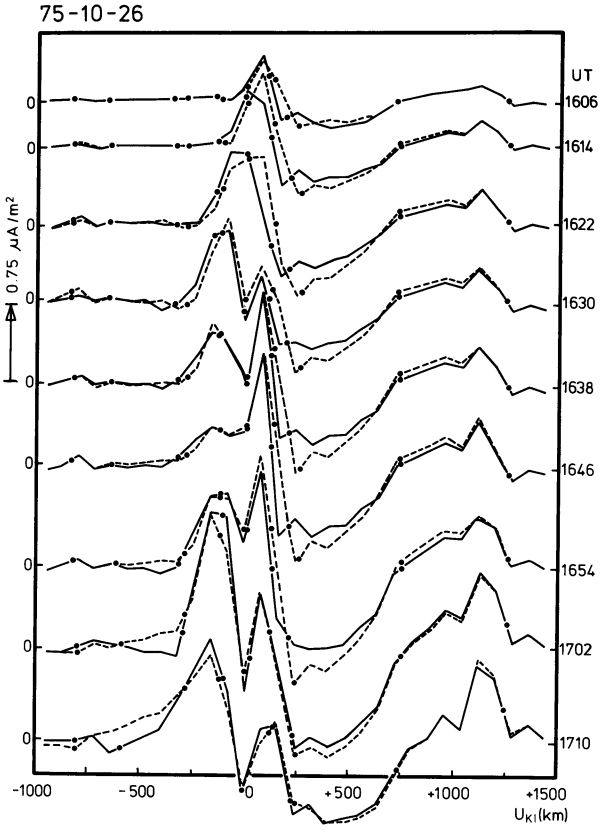

Fig. 7. Latitude profiles of the field-aligned current density derived by differentiating the profiles of Fig. 6. Positive values denote downward currents and vice versa. Otherwise as Fig.. 5

Discussion

The distribution of equivalent height-integrated ionospheric currents and its temporal development derived in this study is in agreement with the results of Kamide and Fukushima (1972) and also consistent with the idea of intrusion of the substorm intensified westward electrojet as introduced by Rostoker and Kisabeth (1973). Wallis et al. (1976) have found a close correlation between the equatorward boundaries of eastward electrojet and diffuse aurora, which Lui et al. (1977) described as the optical image of the inner plasmasheet in the polar ionosphere. Therefore we may relate the equatorward shift of the sharp southern eastward electrojet boundary (see Fig. 6) to an earthward shift of the inner edge of the plasmasheet with increasing activity, which also Winningham et al. (1975) found using Isis observations.

In order to relate the equivalent eastward current to the real ionospheric currents, we have compared the ratio of maximum equivalent height-integrated

eastward current density and maximum northward magnetic variation on the ground with the results of Kamide and Brekke (1975), who compared ionospheric east-west current densities observed by the Chatanika radar with *H*-variations observed at College. We have found good agreement between our ratio (about $2.7 \cdot 10^{-3}$ $Am^{-1}nT^{-1}$) and the ratio which they found for two cases when the center of a slightly stronger current than ours was situated near the Chatanika radar facility. Taking into account that Chatanika observations regularly give a nearly pure northward directed field in the eastward electrojet region (e.g., Wedde et al., 1977; Horwitz et al., 1978) the above mentioned comparison seems to indicate that our technique yields equivalent eastward ionospheric current densities very near to the real eastward Hall-current density when applied to the eastward electrojet. This is consistent with the results of Baumjohann et al. (1978) who found by comparing ground-based magnetometer array data with spatial radar observations that for the eastward electrojet ground-based magnetometers see mainly the effect of the Hall-current flow and magnetic effects of field-aligned and Pedersen-currents cancel each other (Fukushima, 1976).

The large scale configuration of the field-aligned currents observed by us around 1900 MLT is in good agreement with the TRIAD-observations of Iijima and Potemra (1976; 1978) for the same MLT sector and the result of Rostoker et al. (1975). These authors show that field-aligned currents flow downward above both the southern half of the eastward electrojet and the northern half of the westward electrojet region with upward flow in the middle between these two regions. Our field-aligned current densities of about 10^{-6} Am^{-2} are well in the range given by more direct measurements (e.g., Zmuda and Armstrong, 1974; Sugiura and Potemra, 1976) and come very near to the values given by Iijima and Potemra (1978) for their region 1 and 2 currents in this local time sector for disturbed periods. The calculated width of the field-aligned current region (about 1600 km) is greater than that given by Iijima and Potemra (1978) for a substorm expansion phase (about 1000 km) but agrees well with the results of Rostoker et al. (1975).

A really new result found from our present analysis seems to be the small-scale decrease in equivalent eastward ionospheric current density near its maximum. Structures like this have not been reported so far by other authors who used ground-based magnetometer data to model the ionospheric current flow. This is at least partly due to the method of analysis used by these authors, since inverse modelling as used e.g. by Scrase (1967), Czechowsky (1971), and Oldenburg (1976; 1978) needs a forward model of the current density distribution with as few parameters as possible (mostly parabolic or triangular distributions) or a rather smooth latitudinal function to obtain meaningful results.

The local decrease of about 0.1 Am^{-1} (Fig. 6) near the maximum eastward ionospheric current density implies a pair of field-aligned currents of about $4 \cdot 10^{-2}$ Am^{-1} flowing upward in the equatorward and downward on the poleward side of this small-scale structure. Since we have related the equivalent eastward current to a Hall current driven by a pure northward convection electric field, the small-scale field-aligned current pair must have a magnetospheric source. An ionospheric source would require a physically unreasonable decrease in conductivity between the two field-aligned currents to explain the

decrease in eastward current flow (Boström, 1964) and also would yield sheet currents of maximum 10^{-2} Am^{-1} only after Mallinckrodt and Carlson (1978) for polarization electric fields of about 20 mVm^{-1} as given, e.g., by Beaujardiere et al. (1977) for auroral acrs in the evening sector.

We have the strong feeling that the local current sheet pair may be related to an auroral arc. Unfortunately no all-sky camera data was available to prove this, but broad beam riometer recordings made at Tromsø (Stauning and Christensen, 1977) show at least weak precipitation of 10–20 keV electrons in the region of the small-scale structure around 1700 UT when the strongest local sheet currents are observed. This precipitation of energetic electrons is often related to discrete aurora (Wallis, 1976; Evans et al., 1977; Carlson and Kelley, 1977; Lui et al., 1977).

Additional evidence is given by relating our observations to the results of other authors (already reviewed in the introduction to this paper) who observed small-scale structures mostly related to auroral arcs in the eastward electrojet region. The reader may easily see that their observations of structured electron precipitation (Lui et al., 1977; Mende and Eather, 1976), local field-aligned current sheet pairs (Armstrong et al., 1975; Casserly and Cloutier, 1975; Kamide and Rostoker, 1977; Iijima and Potemra, 1978) and southward or strongly decreased northward electric field in or near auroral arcs (Maynard et al., 1977; Evans et al., 1977; Beaujardiere et al., 1977) fit reasonably well to our observations.

We have also compared our results qualitatively with the model of Sato (1978) for quiet auroral arcs, who showed that for an ambient pure northward electric field auroral arcs can develop due to a feedback instability in the coupled ionosphere-magnetosphere system with a local upward current south and a downward sheet current north of the arc, like in our case. He also predicts an arc-associated westward flow of current which should be rather weak if the electric field is only north-south directed, consistent with our observations.

Conclusions and Summary

In the present paper, for the case of an eastward electrojet, we have demonstrated the usefulness of the method of upward continuation (towards the source) for analyzing auroral zone groundbased magnetic observations. This method gives in a rather direct way – as compared to modelling techniques – the density-distribution of the at least equivalent height-integrated ionospheric current. Furthermore, it seems to be capable to reveal rather clearly small-scale (down to 200 km wavelength) structures within the larger scale current flow. Finally, in the present case it allowed for a rather sharp definition of the southward border of the eastward electrojet, this border possibly being related to the inner edge of the magnetospheric plasma sheet.

For the special event which we investigated the more detailed main results have been:

1. Between 1606 and 1702 UT only a two-dimensional analysis was possible both the total value and the maximum density of the eastward flowing height-

integrated equivalent ionospheric current increased by a factor of 5, namely from $4 \cdot 10^4$ to $2 \cdot 10^5$ A, and from 0.1 to 0.5 Am^{-1}, respectively. The demarcation line between the equivalent ionospheric eastward and westward currents remained stationary over this time interval, whereas the well-defined southern border of the eastward current moved towards the south with an average speed of about 50 ms^{-1}, possibly indicating a corresponding movement of the inner edge of the plasma sheet.

2. Under the assumption that the derived equivalent ionospheric current was a pure Hall current, and that the ratio Σ_H/Σ_P was equal to 2 all the time and at all places, the maximum density of the downflowing field-aligned current corresponding to the large-scale eastward electrojet above its southern half was estimated to increase from 0.4 to 1.2 μAm^{-2} over the time interval mentioned. Simultaneously, the broad distribution of upflowing current adjacent to the north showed maximum densities growing from 0.3 to 1.0 μAm^{-2}.

3. A local decrease in eastward electrojet current density probably has been found near its maximum. This implies a local pair (less than 100 km width each) of down- and upflowing field-aligned current sheets with a maximum current density of $0.8 \cdot 10^{-6}$ Am^{-2} and $4 \cdot 10^{-2}$ Am^{-1}, respectively, inside the large-scale region of downflowing current. Evidence has been given that this small-scale structure may possibly be related to a quiet auroral arc.

Acknowledgements. We are greatly indebted to the members of the magnetometer group at the University of Münster, who all were involved collecting the data. We thank especially Professor J. Untiedt for his support during all stages of this work and Dr. A.G. Jones for useful comments on an earlier version of this manuscript. We would like to thank also Drs. Ch. Sucksdorff (Helsinki), S. Berger (Tromsø), F. Eleman (Stockholm), and E. Gjoen (Bergen), who supplied us with the additional magnetic data used in this study. The magnetic observations were performed in cooperation and with much help from the Geophysical Observatory of the Finnish Academy of Sciences and Letters at Sodankylä (Dr. E. Kataja), the Finnish Meteorological Institute at Helsinki (Dr. C. Sucksdorff), the Department of Plasma Physics of the Royal Institute of Technology at Stockholm (Dr. R. Boström, now at Uppsala), the Kiruna Geophysical Institute (Dr. G. Gustafsson), and the Auroral Observatory at Tromsø (Mr. St. Berger). They have been supported financially by grants of the Deutsche Forschungsgemeinschaft. The critical comments and suggestions of two unknown referees have been highly appreciated.

References

Armstrong, J.C., Akasofu, S.-I., Rostoker, G.: A comparison of satellite observations of Birkeland currents with ground observations of visible aurora and ionospheric currents. J. Geophys. Res. **80**, 575–586, 1975

Banks, P.M., Doupnik, J.R., Akasofu, S.-I.: Electric field observations by incoherent scatter radar in the auroral zone. J. Geophys. Res. **78**, 6607–6622, 1973

Baumjohann, W., Greenwald, R.A., Küppers, F.: Joint magnetometer array and radar backscatter observations of auroral currents in Northern Scandinavia. J. Geophys. **44**, 373–383, 1978

Beaujardiere, O. de la, Vondrak, R., Baron, M.: Radar observations of electric fields and currents associated with auroral arcs. J. Geophys. Res. **82**, 5051–5062, 1977

Boström, R.: A model of the auroral electrojets. J. Geophys. Res. **69**, 4983–5000, 1964

Brekke, A., Doupnik, J.R., Banks, P.M.: Incoherent scatter measurements of E-region conductivities and currents in the auroral zone. J. Geophys. Res. **79**, 3773–3790, 1974

Carlson, C.W., Kelley, M.C.: Observation and interpretation of particle and electric field measurements inside and adjacent to an active auroral arc. J. Geophys. Res. **82**, 2349–2360, 1977

Casserly, R.T., Cloutier, P.A.: Rocket-based magnetic observations of auroral Birkeland currents in association with a structured auroral arc. J. Geophys. Res. **80**, 2165–2168, 1975

Czechowsky, P.: Calculation of an equivalent current system in the polar E-region. Radio Sci. **6**, 247–253, 1971

Evans, D.S., Maynard, N.C., Trøim, J., Jacobsen, T., Egeland, A.: Auroral electric field and particle comparisons. 2. Electrodynamics of an arc. J. Geophys. Res. **82**, 2235–2249, 1977

Fukushima, N.: Generalized theorem for no ground magnetic effect of vertical currents connected with Pedersen currents in the uniform-conductivity ionosphere. Rep. Ionos. Space Res. Jpn. **30**, 35–40, 1976

Gough, D.I., Reitzel, J.S.: A portable three component magnetic variometer. J. Geomagn. Geoelectr. **19**, 203–215, 1967

Grant, F.S., West, G.F.: Interpretation theory in applied geophysics. New York: McGraw-Hill 1965

Gustafsson, G.: A revised corrected geomagnetic coordinate system. Ark. Geofys. **5**, 595–617, 1970

Horwitz, J.L., Doupnik, J.R., Banks, P.M.: Chatanika radar observations of the latitudinal distributions of auroral zone electric fields, conductivities, and currents. J. Geophys. Res. **83**, 1463–1481, 1978

Iijima, T., Potemra, T.A.: The amplitude distribution of field-aligned currents at northern high latitudes observed by Triad. J. Geophys. Res. **81**, 2165–2174, 1976

Iijima, T., Potemra, T.A.: Large-scale characteristics of field-aligned currents associated with substorms. J. Geophys. Res. **83**, 599–615, 1978

Kamide, Y., Brekke, A.: Auroral electrojet current density deduced from the Chatanika radar and from the Alaska meridian chain of magnetic observatories. J. Geophys. Res. **80**, 587–594, 1975

Kamide, Y., Brekke, A.: Altitude of the eastward and westward auroral electrojets. J. Geophys. Res. **82**, 2851–2853, 1977

Kamide, Y., Fukushima, N.: Positive geomagnetic bays in evening high-latitudes and their possible connection with partial ring current. Rep. Ionos. Space Res. Jpn. **26**, 79–101, 1972

Kamide, Y., Horwitz, J.L.: Chatanika radar observations of ionospheric and field-aligned currents. J. Geophys. Res. **83**, 1063–1070, 1978

Kamide, Y., Rostoker, G.: The spatial relationship of field-aligned currents and auroral electrojets to the distribution of nightside auroras. J. Geophys. Res. **82**, 5589–5608, 1977

Kertz, W.: Modelle für erdmagnetisch induzierte elektrische Ströme im Untergrund. Nachr. Akad. Wiss. Göttingen 1954, Math.-Phys. Kl., 101–110, 1954

Küppers, F., Post, H.: A second generation Gough-Reitzel magnetometer (accepted for publication). J. Geomagn. Geoelectr. 1979

Küppers, F., Untiedt, J., Baumjohann, W., Lange, K., Jones, A.: A two-dimensional magnetometer array for ground-based observations of auroral zone electric currents during the International Magnetospheric Study (IMS). J. Geophys. 1979

Lui, A.T.Y., Venkatesan, D., Anger, C.D., Akasofu, S.-I., Heikkila, W.J., Winningham, J.D., Burrows, J.R.: Simultaneous observations of particle precipitations and auroral emissions by the Isis 2 satellite in the 19–24 MLT sector. J. Geophys. Res. **82**, 2210–2226, 1977

Mallinckrodt, A.J., Carlson, C.W.: Relations between transverse electric fields and the field-aligned currents. J. Geophys. Res. **83**, 1426–1432, 1978

Maynard, N.C.: Electric field measurements across the Harang discontinuity. J. Geophys. Res. **79**, 4620–4631, 1974

Maynard, N.C., Evans, D.S., Maehlum, B., Egeland, A.: Auroral vector electric field and particle comparisons. 1. Premidnight convection topology. J. Geophys. Res. **82**, 2227–2234, 1977

McNish, A.G.: Heights of electric currents near the auroral zone. Terr. Magn. Atmos. Electr. **43**, 67–75, 1938

Mende, S.B., Eather, R.H.: Monochromatic all-sky observations and auroral precipitation patterns. J. Geophys. Res. **81**, 3771–3780, 1976

Oldenburg, D.W.: Ionospheric current structure as determined from groundbased magnetometer data. Geophys. J. **46**, 41–66, 1976

Oldenburg, D.W.: A quantitative technique for modelling ionospheric and magnetospheric current distributions. J. Geophys. Res. **83**, 3320–3326, 1978

Rostoker, G.: Polar magnetic substorms. Rev. Geophys. Space Phys. **10**, 157–211, 1972
Rostoker, G., Armstrong, J.C., Zmuda, A.J.: Field-aligned current flow associated with intrusion of the substorm-intensified westward electrojet into the evening sector. J. Geophys. Res. **80**, 3571–3579, 1975
Rostoker, G., Kisabeth, J.L.: Response of the polar electrojets in the evening sector to polar magnetic substorms. J. Geophys. Res. **78**, 5559–5571, 1973
Sato, T.: A theory of quiet auroral arcs. J. Geophys. Res. **83**, 1042–1048, 1978
Scrase, F.J.: The electric current associated with polar magnetic sub-storms. J. Atmos. Terr. Phys. **29**, 567–579, 1967
Siebert, M., Kertz, W.: Zur Zerlegung eines lokalen erdmagnetischen Feldes in äußeren und inneren Anteil. Nachr. Akad. Wiss. Göttingen 1957, Math.-Phys. Kl., 87–112, 1957
Stauning, P., Christensen, B.: Compilation of Ionlab riometer data for IMS-Workshop in Hankasalmi. Ionlab Rep. R41, Lyngby (Denmark), 1977
Sugiura, M., Potemra, T.A.: Net field-aligned currents observed by Triad. J. Geophys. Res. **81**, 2155–2164, 1976
Untiedt, J., Pellinen, R., Küppers, F., Opgenoorth, H.J., Pelster, W.D., Baumjohann, W., Ranta, H., Kangas, J., Czechowsky, P., Heikkila, W.J.: Observations of the initial development of an auroral and magnetic substorm at magnetic midnight. J. Geophys. **45**, 41–65, 1978
Wallis, D.D.: Comparison of auroral electrojets and the visible aurora. In: Magnetospheric particles and fields, B.M. McCormack, ed., pp. 247–255. Dordrecht: D. Reidel 1976
Wallis, D.D., Anger, C.D., Rostoker, G.: The spatial relationship of auroral electrojets and visible aurora in the evening sector. J. Geophys. Res. **81**, 2857–2869, 1976
Weaver, J.T.: On the separation of local geomagnetic fields into external and internal parts. Z. Geophys. **30**, 29–36, 1964
Wedde, T., Doupnik, J.R., Banks, P.M.: Chatanika observations of the latitudinal structure of electric fields and particle precipitation on November 21, 1975. J. Geophys. Res. **82**, 2743–2751, 1977
Wescott, E.M., Stolarik, J.D., Heppner, J.P.: Electric fields in the vicinity of auroral forms from motions of barium vapor releases. J. Geophys. Res. **74**, 3469–3487, 1969
Winningham, J.D., Yasuhara, F., Akasofu, S.-I., Heikkila, W.J.: The latitudinal morphology of 10-eV to 10-keV electron fluxes during magnetically quiet and disturbed times in the 2100–0300 MLT sector. J. Geophys. Res. **80**, 3148–3171, 1975
Zmuda, A.J., Armstrong, J.C.: The diurnal flow pattern of field-aligned currents. J. Geophys. Res. **79**, 4611–4619, 1974

Received January 11, 1979; Revised Version April 3, 1979; Accepted April 4, 1979